

# Frustration, Chaos, and Order in the $d=1$ Ising Spin Glass with Long-Range Power-Law Interactions

E. Can Artun<sup>1,2</sup> and A. Nihat Berker<sup>2,3</sup>

<sup>1</sup>*TUBITAK Research Institute for Fundamental Sciences (TBAE), Gebze, Kocaeli 41470, Turkey*

<sup>2</sup>*Faculty of Engineering and Natural Sciences, Kadir Has University, Cibali, Istanbul 34083, Turkey*

<sup>3</sup>*Department of Physics, Massachusetts Institute of Technology, Cambridge, Massachusetts 02139, USA*

The  $d = 1$  Ising spin glass with long-range power-law interactions  $Jr^{-\alpha}$  is studied for all  $\alpha$  by a renormalization-group transformation that simultaneously projects local ferromagnetism and antiferromagnetism. In the ferromagnetic case,  $J > 0$ , a finite-temperature ferromagnetic phase occurs for  $0.75 < \alpha < 2$ . The transition temperature monotonically decreases between these two limits. At  $\alpha = 2$ , the phase-transition temperature discontinuously drops to zero and for  $\alpha > 2$  there is no ordered phase above zero temperature, as predicted by rigorous results. On approaching  $\alpha = 0.75$  from above, the phase-transition temperature diverges to infinity, meaning that, at all temperatures above zero, the system is ferromagnetically ordered. Thus, the equivalent-neighbor interactions regime is entered before ( $\alpha \neq 0$ ) the neighbors become equivalent, namely before the interaction become equal for all separations. The critical exponents are calculated, from a large recursion matrix, as a function of  $\alpha$ . For the antiferromagnetic case,  $J < 0$ , all triplets of spins have competing interactions and this highly frustrated system does not have an ordered phase. In the spin-glass phase, where all couplings for all separations are randomly ferromagnetic or antiferromagnetic (with probability  $p$ ), a finite-temperatures phase diagram is obtained with order in the presence of frustration. Transient chaos is found within the ferromagnetic phase.

## I. CONTINUOUSLY VARIABLE CRITICAL EXPONENTS IN THE XY ASHKIN-TELLER COMPLEXITY

### A. Ashkin-Tellerized XY Model

A distinctive low-temperature phase which actually is a continuously varying continuum of critical points, with absence of length scale, is seen in spatial dimension  $d = 2$  in the XY model [? ? ? ? ? ? ? ? ? ?],

$$-\beta\mathcal{H} = \sum_{\langle ij \rangle} J \vec{s}_i \cdot \vec{s}_j, \quad (1)$$

where  $\beta = 1/k_B T$  is the inverse temperature, at each site  $i$  there is an XY unit spin  $\vec{s}_i$  that can point in an angle between 0 and  $2\pi$ , and the sum is over all pairs of spins on nearest-neighbor sites.

On the other hand, the conventional Ashkin-Teller model [? ? ?] is a doubled-up progeny of the up-down discrete spin Ising model, ushering a multiplicity of order parameters and ordered phases from this discrete-spin model. Using continuously orientable XY spins instead of discrete Ising spins, with the algebraic ordering of  $d = 2$ , brings a multiplicity of algebraic orders. This XY Ashkin-Teller model is defined by the Hamiltonian

$$\begin{aligned} -\beta\mathcal{H} &= \sum_{\langle ij \rangle} [J(\vec{s}_i \cdot \vec{s}_j + \vec{t}_i \cdot \vec{t}_j) + M(\vec{s}_i \cdot \vec{s}_j)(\vec{t}_i \cdot \vec{t}_j)] \\ &= \sum_{\langle ij \rangle} -\beta\mathcal{H}_{ij}(\vec{s}_i, \vec{t}_i; \vec{s}_j, \vec{t}_j), \quad (2) \end{aligned}$$

where at each site  $i$  there are two XY unit spins  $\vec{s}_i, \vec{t}_i$  that can point in an angle between 0 and  $2\pi$ , and the

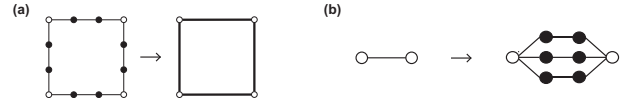


FIG. 1. Exact solution of  $d = 2$  hierarchical model and Migdal-Kadanoff: (a) The Migdal-Kadanoff approximate renormalization-group transformation on the square lattice. Bonds are removed from the square lattice to make the renormalization-group transformation doable. The removed bonds are compensated by adding their effect to the decimated remaining bonds. (b) A hierarchical model is constructed by self-embedding a graph into each of its bonds, *ad infinitum*. [9] The exact renormalization-group solution proceeds in the reverse direction, by summing over the internal spins shown with the dark circles. Here is the most used, so called "diamond" hierarchical lattice [9–12]. The length-rescaling factor  $b$  is the number of bonds in the shortest path between the external spins shown with the open circles,  $b = 3$  in this case. The volume rescaling factor  $b^d$  is the number of bonds replaced by a single bond,  $b^d = 9$  in this case, so that  $d = 2$ .

sum is over all interacting quadruples of spins on nearest-neighbor pairs of sites.

A thermodynamic phase with algebraic order [? ? ? ? ? ? ? ? ? ?] does not have a non-zero order parameter such as a magnetization, but is characterized by long-range algebraically decaying correlations, such as a spin-spin correlation function, as opposed to an exponentially decaying correlation function. The algebraically ordered phase has no physical length scale (therefore no exponentially decaying correlation function, since there is no physical length to divide the length variable in the exponent). In fact, an algebraically ordered phase can be seen as a continuum of critical points, with continuously vary-

ing critical exponents (resulting from a renormalization-group fixed line) or with uniform critical exponents (resulting from a finite-temperature phase-sink fixed point). Algebraically ordered phases occur: in  $d = 2$ , in XY spin systems, solids, liquid crystals [? ? ? ? ? ?] and, in a variety of  $d$ , in antiferromagnetic Potts models [? ? ?].

### B. Semi-Infinite Quasi-Disorder Lines

Considering the aligned and anti-aligned spin states, also as representatives for continuous deviations from these states, on the semi-infinite line  $M = J < 0$ , twelve of the sixteen possible states of  $(s_i, t_i, s_j, t_j)$  have the lowest interaction energy  $\beta\mathcal{H} = J < 0$ , whereas the other four states have energy  $\beta\mathcal{H} = -3J > 0$ , with a gap of  $4J$ . These four states contribute less and less as temperature is lowered (i.e., as  $J$  is increased). Thus, on the  $J = M < 0$  semi-infinite line, there is a twelvefold ground-state degeneracy and this line is a quasi-disorder line: If all sixteen spin states had the same energy, no ordering would occur in this totally degenerate system. Nevertheless, in the current situation of twelve degenerate ground states and four less participating high energy states, the lack of ordering can be anticipated. Thus we call this semi-infinite line a quasi-disorder line [?] and, in fact, no ordering occurs, as seen below.

The same happens along the semi-infinite line  $-M = J > 0$ , which is therefore also a quasi-disorder line. We shall see that the disordered phase hugs these two quasi-disorder lines all the way to infinite interactions, i.e., zero temperature.

## II. METHOD: RENORMALIZATION-GROUP TRANSFORMATION OF THE DOUBLE FOURIER EXPANSION OF TWO CONTINUOUS ANGLES

The renormalization-group transformation, explained in Fig. 1, is done with length rescaling factor  $b = 3$ , an odd number in order to conserve the ferromagnetic-antiferromagnetic symmetry of the method.[8] This method [?] involves decimating three bonds in series into a single bond, followed by bond-moving by superimposing  $b^{d-1} = 3$  bonds. This approach is an approximate solution on the  $d = 2$  square lattice and, simultaneously, an exact solution on the  $d = 2$  hierarchical lattice [9–12]. The simultaneous exact solution makes the approximate solution a physically realizable, therefore robust approximation. Physically realizable approximations have been used in studies of turbulence [13], polymers [14], gels [15], electronic systems [16]. For recent works on hierarchical lattices, see Refs.[20–35]

As seen in Fig. 1, the first step of the renormalization-group transformation involves decimation over three consecutive bonds. We give below the decimation of two

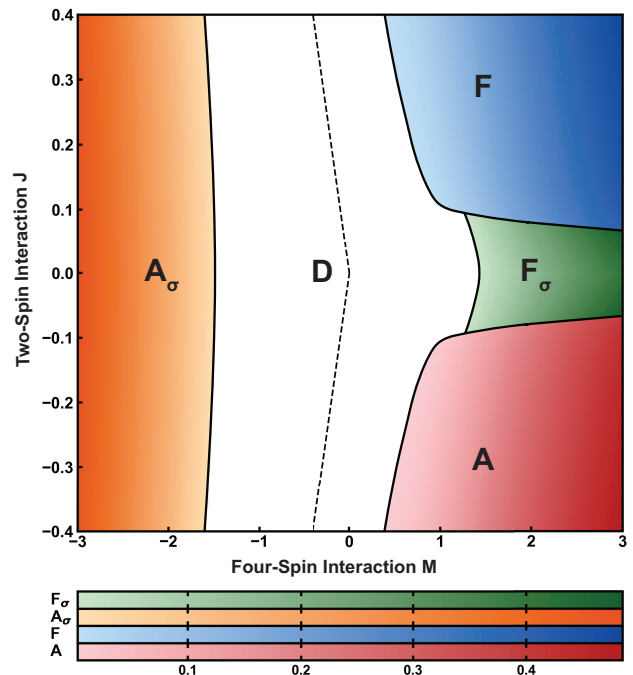


FIG. 2. Calculated phase diagram of the XY Ashkin-Teller model in spatial dimension  $d = 2$ . The ferromagnetic ( $F$ ) and antiferromagnetic ( $A$ ) phases of the continuously orientable spin variables  $\vec{s}_i$  and  $\vec{t}_i$ , the ferromagnetic ( $F_\sigma$ ) and antiferromagnetic ( $A_\sigma$ ) phases of the composite spin variable  $\vec{s}_i\vec{t}_i$ , and the disordered phase ( $D$ ) are shown. The color intensity shows the continuously varying criticality of the algebraically ordered phases, by the mechanism of trajectories starting at different points in the phase diagram reaching different points on the fixed line. The critical exponents are evaluated by calculating the derivative matrix of the renormalization-group recursion matrix. In this case, this would be the recursion of the Fourier coefficients. Such a determination, done at various points on the fixed line, yields continuously varying critical exponents [?]. Thus, this color intensity indicates the numerical value of, taken for example, the double Fourier coefficients  $f(2, 2)$  of the final destination, on the fixed line, of the renormalization-group trajectory starting at the phase diagram point. The dashed semi-infinite lines show the *a priori* quasi-disorder lines. The disordered phase  $D$  hugs the quasi-disorder lines all the way to infinite-strength interactions, namely zero temperature.

consecutive bonds. Decimating the result of this with another (undecimated) bond gives the decimation of three consecutive bonds.

A decimated bond is obtained by integrating over the shared two spins of two bonds. With  $u_{ij}(\theta_{ij}, \varphi_{ij}) = e^{-\beta\mathcal{H}_{ij}(\vec{s}_i, \vec{t}_i; \vec{s}_j, \vec{t}_j)}$  being the exponentiated nearest-neighbor Hamiltonian between sites  $(i, j)$ , and  $\theta_{ij} = \theta_i - \theta_j$  and  $\varphi_{ij} = \varphi_i - \varphi_j$  being the angles between the planar unit vectors  $(\vec{s}_i, \vec{s}_j)$  and  $(\vec{t}_i, \vec{t}_j)$ , as defined af-

ter Eq.[2], decimation proceeds as

$$\tilde{u}_{13}(\theta_{13}, \varphi_{13}) = \int_0^{2\pi} u_{12}(\theta_{12}, \varphi_{12}) u_{23}(\theta_{23}, \varphi_{23}) \frac{d\theta_2}{2\pi} \frac{d\varphi_2}{2\pi}. \quad (3)$$

On the left side of this equation, tilde  $\sim$  means decimated. Using a double Fourier transformation,

$$f(k, l) = \int_0^{2\pi} u(\theta, \varphi) e^{ik\theta + il\varphi} \frac{d\theta}{2\pi} \frac{d\varphi}{2\pi},$$

$$u(\theta, \varphi) = \sum_{k=-\infty}^{\infty} \sum_{l=-\infty}^{\infty} e^{-ik\theta - il\varphi} f(k, l), \quad (4)$$

the decimation of Eq.(3) becomes

$$\tilde{f}_{13}(k, l) = f_{12}(k, l) f_{23}(k, l). \quad (5)$$

Here  $f_{ij}(k, l)$  are the Fourier coefficients for the interaction between sites  $i$  and  $j$ .

As also seen in Fig. 1, the second step of the renormalization-group transformation involves bond moving three bonds. We give below the bond moving of two bonds. Moving onto the result of this another (unmoved) bond gives the bond moving of three bonds.

Bond moving bonds  $(i_1 j_1)$  and  $(i_2 j_2)$  to obtain bond  $(ij)$  is effected as

$$u'_{ij}(\theta, \varphi) = \tilde{u}_{i_1 j_1}(\theta, \varphi) \tilde{u}_{i_2 j_2}(\theta, \varphi),$$

$$f'_{ij}(k, l) = \sum_{m=-\infty}^{\infty} \sum_{n=-\infty}^{\infty} \tilde{f}_{i_1 j_1}(k - m, l - n) \tilde{f}_{i_2 j_2}(m, n). \quad (6)$$

On the left side of this equation, prime means bond-moved.

We have followed the renormalization-group flows in terms of the  $k = 0$  to 20 and  $l = 0$  to 20 double Fourier components, thus having 441 renormalization-group flow quantities, and also using  $f_{ij}(k, l) = f_{ij}(-k, l) = f_{ij}(k, -l) = f_{ij}(-k, -l)$ . We also made spot checks with higher number of double Fourier components (up to  $k, l = 0$  to 100). The spot checks have yielded no differences, to the accuracy of the thickness of the lines in our figures. This is also the case in [? ?]. We set to unity the maximum value of the double Fourier components, by dividing with the same constant (the raw maximal value), which amounts to adding the same constant to all energies.

### III. RESULTS: PHASE DIAGRAM AND QUADRUPLE RENORMALIZATION-GROUP FIXED LINES OF POTENTIAL SURFACES

The phase diagram (Fig. 2) is obtained by following the renormalization-group flows of the double Fourier coefficients  $f(k, l)$ , obtained as described above, respectively to their stable fixed lines and stable fixed point

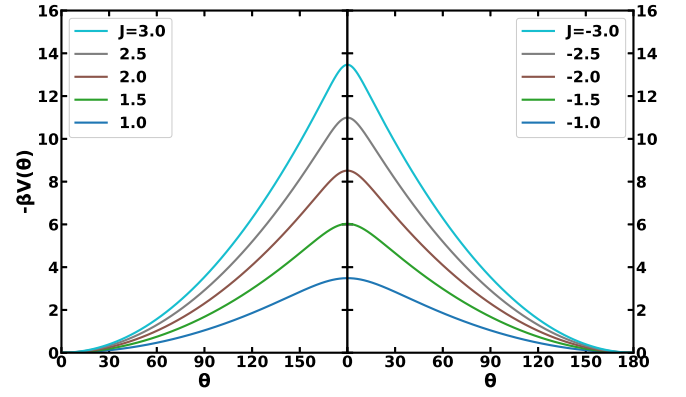


FIG. 3. Renormalization-group trajectory terminal energy functions in the algebraically ordered phases of the single XY model, in the ferromagnetic (left panel) and antiferromagnetic (right panel) phases. The negative logarithm  $\beta V(\theta) = -\ln(u)$  of the multiply renormalized exponentiated nearest-neighbor energy  $u_{XY} = e^{-\beta \mathcal{H}_{ij}(\vec{s}_i; \vec{s}_j)}$  is shown, as an energy as a function of the angle  $\theta$  between the spins  $\vec{s}_i, \vec{s}_j$ . For each energy curve, the starting spin-spin coupling  $J$  is indicated, from top to bottom. The continuum of such curves constitutes the fixed-line sink [36] of the algebraically ordered phase.

( $D$ ), namely sinks. The basin of attraction of each sink is a corresponding thermodynamic phase.[36] In this XY-Ashkin-Teller model, there are five sinks and therefore five distinct thermodynamic phases. The spin-spin interactions deduced from the exponentiated nearest-neighbor interactions,  $u_{ij}(\theta_{ij}, \varphi_{ij}) = e^{-\beta \mathcal{H}_{ij}(\vec{s}_i, \vec{t}_i; \vec{s}_j, \vec{t}_j)}$ , reconstructed [Eq.(4)] from the double Fourier coefficients, at four of these sinks are shown below. A sink epitomizes the ordering of its corresponding thermodynamic phase that it attracts under renormalization group.

The sinks of the renormalization-group flows, for the four ordered phases (Fig. 2) in this system, are fixed lines of potential surfaces that are determined by the terminal fixed values of the double Fourier coefficients  $f(k, l)$ . At the ordered sinks (but not in the flows leading to the sinks), the double Fourier coefficient factorizes. For example, at the sink of the ferromagnetic phase  $F$ ,

$$f(k, l) = f(k) f(l), \quad (7)$$

where  $f(k)$  are the Fourier coefficients at the ferromagnetic sink of a single XY model, given in the left panel of Fig. 3. This factorization, and the factorizations given below, only occur at the fixed surfaces, but not in the renormalization-group flows from any system with  $M \neq 0$ . At the sink of the antiferromagnetic phase  $A$ ,

$$f(k, l) = f^A(k) f^A(l), \quad (8)$$

where  $f^A(k) = (-1)^k f(k)$  are the Fourier coefficients at the antiferromagnetic fixed-line sink of a single XY model, given in the right panel of Fig. 3. At the sink of the locked-spin ferromagnetic phase  $F_\sigma$ ,

$$f(k, l) = f_L(k) f_L(l), \quad (9)$$

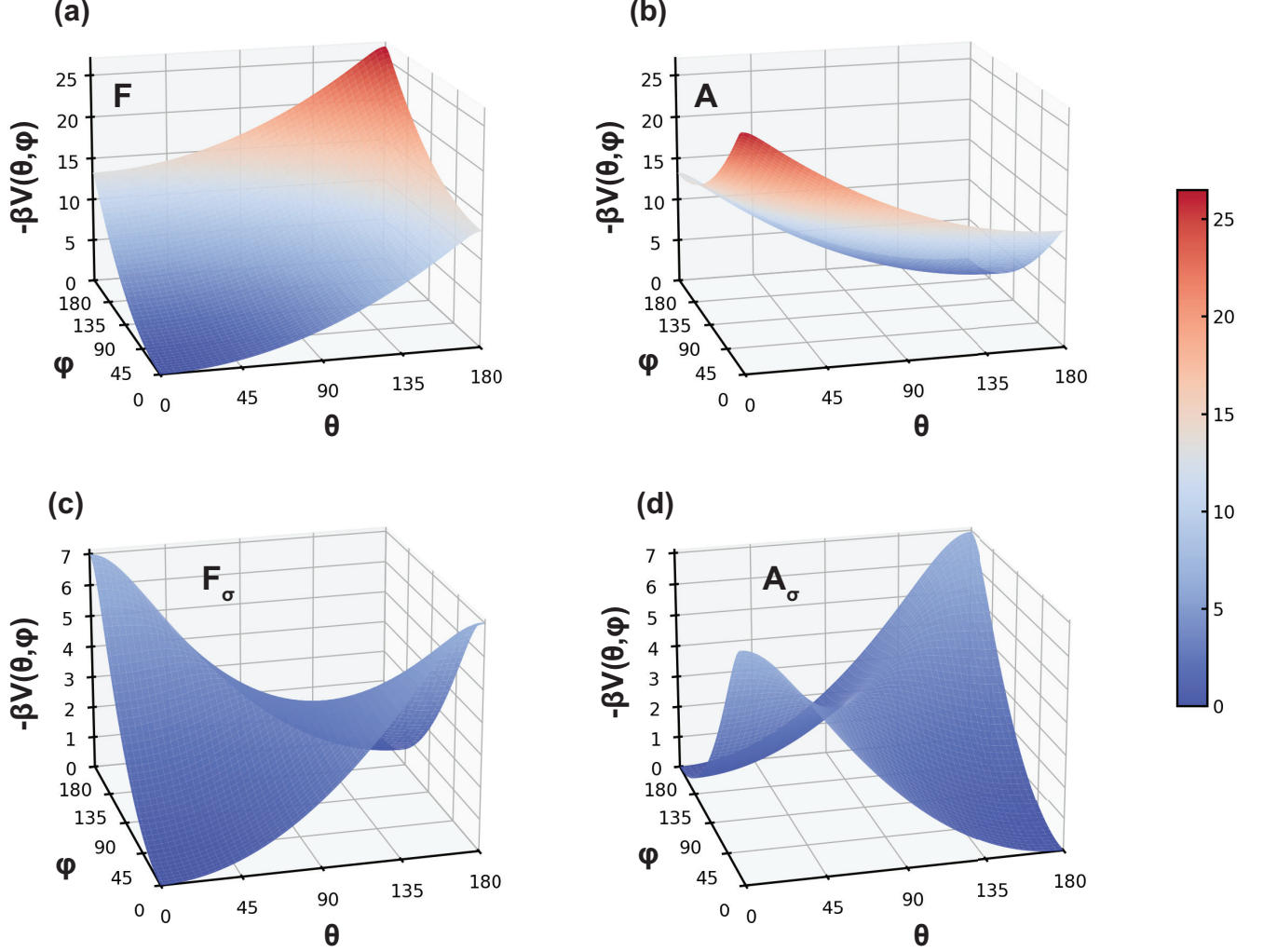


FIG. 4. Potential functions on the fixed lines of the renormalization-group sinks of the (a) ferromagnetic phase  $F$ , (b) antiferromagnetic phase  $A$ , (c) locked ferromagnetic phase  $F_\sigma$ , (d) locked antiferromagnetic phase  $A_\sigma$  of the XY Ashkin-Teller model. The potential function, namely the negative logarithm  $\beta V(\theta, \phi) = -\ln(u)$  of the exponentiated nearest-neighbor energy  $u = e^{-\beta \mathcal{H}_{ij}(\vec{s}_i, \vec{t}_i; \vec{s}_j, \vec{t}_j)}$  is shown, as a function of the angle  $\theta$  between the spins  $\vec{s}_i, \vec{s}_j$  and the angle  $\phi$  between the spins  $\vec{t}_i, \vec{t}_j$ . The starting couplings of the renormalization-group trajectories leading to these potentials are  $(J, M) = (2, 1), (-2, 1), (0.02, 2), (0.1, -2)$  for (a),(b),(c),(d) respectively.

where  $f_L(k)$  are the Fourier coefficients of the ferromagnetic coupling between combination neighboring angles  $(\theta_{ij} + \varphi_{ij})/2$ . At the sink of the locked-spin antiferromagnetic phase  $A_\sigma$ ,

$$f(k, l) = f_L^A(k) f_L^A(l), \quad (10)$$

where  $f_L^A(k)$  are the Fourier coefficients of the antiferromagnetic coupling between combination neighboring angles  $(\theta_{ij} - \varphi_{ij})/2$ .

The potential functions resulting from these double Fourier coefficients are shown in Fig. 3, 4. Thus, at the sink of the ferromagnetic phase  $F$ , the  $\vec{s}_i$  spins are aligned,  $(\theta_{ij} = 0)$ , with each other and separately the  $\vec{t}_i$  spins are aligned,  $(\varphi_{ij} = 0)$ , with each other. At the sink of the antiferromagnetic phase  $A$ , the neighboring  $\vec{s}_i$  spins are antialigned,  $(\theta_{ij} = \pi)$ , with each other and separately the neighboring  $\vec{t}_i$  spins are antialigned,  $(\varphi_{ij} = \pi)$ , with each other. At the sink of



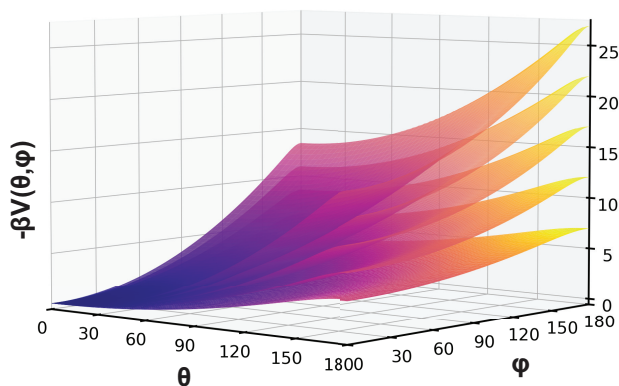


FIG. 5. Examples of potential functions on the fixed line of the renormalization-group sink of the ferromagnetic phase  $F$ ,  $\beta V(\theta, \phi) = -\ln(u)$  of the exponentiated nearest-neighbor energy  $u = e^{-\beta \mathcal{H}_{ij}(\vec{s}_i, \vec{t}_i; \vec{s}_j, \vec{t}_j)}$ . The various fixed energy surfaces are reached from different initial couplings  $(J, M)$ . In this figure, from bottom to top, the initial couplings are  $(J, M) = (1, 0.1), (1.5, 0.1), (2, 0.1), (2.5, 0.1), (3, 0.1)$ .

the locked ferromagnetic phase  $F_\sigma$ , the neighboring spins  $\vec{s}_i = \pm \vec{s}_j$  and simultaneously  $\vec{t}_i = \pm \vec{t}_j$ , the upper (or lower) signs being jointly valid,  $\theta_{ij}, \varphi_{ij} = 0$  or  $\pi$ . At the sink of the locked antiferromagnetic phase, in neighboring  $(s_i, s_j)$  and  $(t_i, t_j)$  are either respectively aligned and antialigned, or respectively antialigned and aligned.

The latter two ordered phases have an entropy per bond  $S/N = \ln 2$ . Furthermore, in all four ordered phases, the relative orientation of the  $s_i$  and  $t_i$  systems has a global degeneracy of  $2\pi$ . The sink of the disordered phase  $D$  has the  $(0,0)$  double Fourier coefficient equal to unity, all other double Fourier coefficients equal to zero. Therefore,  $u_{ij}(\theta_{ij}, \varphi_{ij}) = e^{-\beta \mathcal{H}_{ij}(\vec{s}_i, \vec{t}_i; \vec{s}_j, \vec{t}_j)} = 1$  and  $\beta V(\theta, \varphi) = 0$  independent of angle.

#### IV. CONCLUSION

We have solved, by renormalization-group theory, the Ashkin-Teller type doubled-up XY magnetic spin model in spatial dimension  $d = 2$ . We find four different ordered phases, with ferromagnetic and antiferromagnetic orderings of the direct and composite spins. All four ordered phases have algebraic order, subtended renormalization-group fixed lines of potential surfaces. The disordered phase occurs around two semi-infinite *a priori* quasi-disorder lines, down to zero temperature (infinite coupling).

#### ACKNOWLEDGMENTS

Support by the Academy of Sciences of Turkey (TÜBA) is gratefully acknowledged.

- 
- [1] R. B. Griffiths
  - [2] D. Ruelle
  - [3] D. J. Thouless
  - [4] M. Aizenman
  - [5] M. Aizenman
  - [6] G. Grinstein, A. N. Berker, J. Chalupa, and M. Wortis, Phys. Exact Renormalization Group with Griffiths Singularities and Spin-Glass Behavior: The Random Ising Chain, Phys. Rev. Lett. **36**, 1508 (1976).
  - [7] Th. Niemeijer and J. M. J. van Leeuwen, Physica (Utr.) **71**, 17 (1974).
  - [8] J. M. J. van Leeuwen, Singularities in the Critical Surface and Universality for Ising-Like Spin Systems, Phys. Rev. Lett. **34**, 1056 (1975).
  - [9] A. N. Berker and S. Ostlund, Renormalisation-group calculations of finite systems: Order parameter and specific heat for epitaxial ordering, J. Phys. C **12**, 4961 (1979).
  - [10] R. B. Griffiths and M. Kaufman, Spin systems on hierarchical lattices: Introduction and thermodynamic limit, Phys. Rev. B **26**, 5022R (1982).
  - [11] M. Kaufman and R. B. Griffiths, Spin systems on hierarchical lattices: 2. Some examples of soluble models, Phys. Rev. B **30**, 244 (1984).
  - [12] A. N. Berker and S. R. McKay, Hierarchical Models and Chaotic Spin Glasses, J. Stat. Phys. **36**, 787 (1984).
  - [13] R. H. Kraichnan, Dynamics of Nonlinear Stochastic Systems, J. Math. Phys. **2**, 124 (1961).
  - [14] P. J. Flory, Principles of Polymer Chemistry (Cornell University Press: Ithaca, NY, USA, 1986).
  - [15] M. Kaufman, Entropy Driven Phase Transition in Polymer Gels: Mean Field Theory, Entropy **20**, 501 (2018).
  - [16] P. Lloyd and J. Oglesby, Analytic Approximations for Disordered Systems, J. Phys. C: Solid St. Phys. **9**, 4383 (1976).
  - [17] L. P. Kadanoff, Phys. Rev. Lett. **34**, 1005 (1975).
  - [18] L. P. Kadanoff and A. Houghton, Phys. Rev. B **11**, 377 (1975).
  - [19] L. P. Kadanoff, A. Houghton, and M. C. Yalabık, J. Stat. Phys. **14**, 171 (1976).
  - [20] E. C. Artun, D. Sarman, and A. N. Berker, Nematic Phase of the n-Component Cubic-Spin Spin Glass in  $d=3$ : Liquid-Crystal Phase in a Dirty Magnet, Physica A **40**, 129709 (2024).
  - [21] Y. E. Pektaş, E. C. Artun, and A. N. Berker, Driven and Non-Driven Surface Chaos in Spin-Glass Sponges, Chaos, Solitons and Fractals **17**, 114159 (2023).
  - [22] Y. H. Zhang, J. Y. Qiao, and J. Y. Gao, Feigenbaum Julia Sets Concerning Renormalization Transformation, Frontiers Math. **20**, 185 (2025).
  - [23] S. S. Akimenko and A. Myshlyavtsev, Tensor Networks for Hierarchical Lattices, European Phys. Lett. **148**, 61001 (2024).
  - [24] J. Clark and C. Lochridge, Weak-disorder limit for directed polymers on critical hierarchical graphs with vertex disorder, Stochastic Processes Applications **158**, 75

- (2023).
- [25] M. Kotorowicz and Y. Kozitsky, Phase transitions in the Ising model on a hierarchical random graph based on the triangle, *J. Phys. A* **55**, 405002 (2022).
  - [26] P. P. Zhang, Z. Y. Gao, Y. L. Xu, C. Y. Wang, and X. M. Kong, Phase diagrams, quantum correlations and critical phenomena of antiferromagnetic Heisenberg model on diamond-type hierarchical lattices, *Quantum Science Technology* **7**, 025024 (2022).
  - [27] K. Jiang, J. Qiao, and Y. Lan, Chaotic Renormalization Flow in the Potts model induced by long-range competition, *Phys. Rev. E* **103**, 062117 (2021).
  - [28] G. Mograby, M. Derevyagin, G. V. Dunne, and A. Teplyaev, Spectra of perfect state transfer Hamiltonians on fractal-like graphs, *J. Phys. A* **54**, 125301 (2021).
  - [29] I. Chio, R. K. W. Roeder, Chromatic zeros on hierarchical lattices and equidistribution on parameter space, *Annales de l'Institut Henri Poincaré D*, **8**, 491 (2021).
  - [30] B. Steinhurst and A. Teplyaev, Spectral analysis on Barlow and Evans' projective limit fractals, *J. Spectr. Theory* **11**, 91 (2021).
  - [31] A. V. Myshlyavtsev, M. D. Myshlyavtseva, and S. S. Aki-menko, Classical lattice models with single-node interactions on hierarchical lattices: The two-layer Ising model, *Physica A* **558**, 124919 (2020).
  - [32] M. Derevyagin, G. V. Dunne, G. Mograby, and A. Teplyaev, Perfect quantum state transfer on diamond fractal graphs, *Quantum Information Processing*, **19**, 328 (2020).
  - [33] S.-C. Chang, R. K. W. Roeder, and R. Shrock, q-Plane zeros of the Potts partition function on diamond hierarchical graphs, *J. Math. Phys.* **61**, 073301 (2020).
  - [34] C. Monthus, Real-space renormalization for disordered systems at the level of large deviations, *J. Stat. Mech. - Theory and Experiment*, 013301 (2020).
  - [35] O. S. Sariyer, Two-dimensional quantum-spin-1/2 XXZ magnet in zero magnetic field: Global thermodynamics from renormalisation group theory, *Philos. Mag.* **99**, 1787 (2019).
  - [36] A. N. Berker and M. Wortis, Blume-Emery-Griffiths-Potts Model in Two Dimensions: Phase Diagram and Critical Properties from a Position-Space Renormalization Group, *Phys. Rev. B* **14**, 4946 (1976).